

DARK CURRENT SIMULATIONS FOR THE CORNELL ERL

C.E. Mayes, C. Chiu, G.H. Hoffstaetter, V.O. Kostroun, L.M. Nash, D.C. Sagan
CLASSE, Cornell University, Ithaca NY 14853 USA

Abstract

Charged particles unintentionally transported through an accelerator, collectively called the dark current, can be lost in the beam chamber and create a radiation hazard for both equipment and personnel. Here we simulate the creation of particles by field emission in the superconducting accelerating cavities of the Cornell Energy Recovery Linac, and track them to their loss points. These lost particles can then be used to simulate background radiation. The presented calculations are therefore an essential step in the design of appropriate radiation-shielding of components around the linac.

INTRODUCTION

The Cornell Energy Recovery Linac (ERL) will accelerate electrons up to 5 GeV, use them to produce undulator radiation, and decelerate them to recover their energy [1]. It does this using two linacs separated by a turn-around arc which house a total of 384 superconducting accelerating cavities. Because of the high surface electric fields in these cavities, contamination of, or defects in, the cavity walls can lead to the production of field emitted electrons, which are transported and lost elsewhere in the machine [2]. These currents can heat and damage the beam pipe and cavity walls, damage nearby electronics, demagnetize permanent magnets, and lead to neutron production and other radiation [3, 4, 5, 6].

SIMULATION

The Cornell ERL lattice has been designed primarily using the Bmad particle simulation software library [7]. Like many accelerator codes, Bmad typically tracks particles in curvilinear coordinates with a reference path length s as the independent variable. While well-suited for the designed particle beam, tracking with such a coordinate system fails when particles turn around within a lattice element.

In order to track arbitrary particles, we have developed a Bmad module that uses curvilinear coordinates with time t as the independent variable [8]. The routines in this module are able to import a particle at an arbitrary location and time within the lattice, integrate its trajectory in time, and find the location on the beam pipe or cavity wall that it is lost at. For accelerating cavities, the electric and magnetic fields in the entire bulk of the cavity (calculated externally) are tabulated and used for this tracking. This general purpose tracker have been benchmarked against the simulation code OPAL [9].

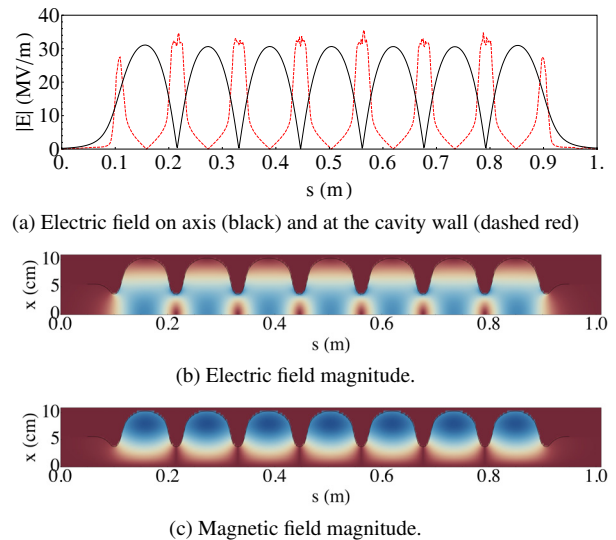


Figure 1: Calculated fields in the Cornell ERL 7-cell SRF accelerating cavity, oscillating at 1.3 GHz.

With the ability to track particles in time, we produced test particles that represent likely field emission points within the cavities. The current from a single field emitter is modeled by the Fowler-Nordheim equation,

$$I_{\text{FN}}(E_{\perp}) = a_0 A_{\text{FN}} (\beta_{\text{FN}} E_{\perp})^2 \exp\left(-\frac{a_1}{\beta_{\text{FN}} E_{\perp}}\right), \quad (1)$$

with factors $a_0 = 3.85 \times 10^{-7} \text{ A/V}^2$ and $a_1 = 5.464 \times 10^{10} \text{ V/m}$ for a Nb cavity [6]. E_{\perp} is the magnitude of the electric field component perpendicular to the surface, and this equation is valid only when the force from this field points away from the surface. The parameters A_{FN} and β_{FN} are interpreted as the effective area and field enhancement factor for the emitter, and can be fitted empirically to a given measured emitter.

In order to sample field emission in an entire cavity, test particles are placed in equally spaced intervals along the contour of the cavity wall. Because we assume cylindrical symmetry in this geometry, each particle is given a random angle in the transverse plane. The charge Q_n that the n^{th} particle represents, placed on the cavity wall at time t_n , is

$$Q_n = N_A \cdot A_n \cdot \frac{\Delta\phi_n}{2\pi f_{\text{rf}}} \cdot I_{\text{FN}}(E_{\perp}(t_n)), \quad (2)$$

where $\Delta\phi_n$ and A_n are the RF phase interval and surface area that the particle represents, N_A is the number of field

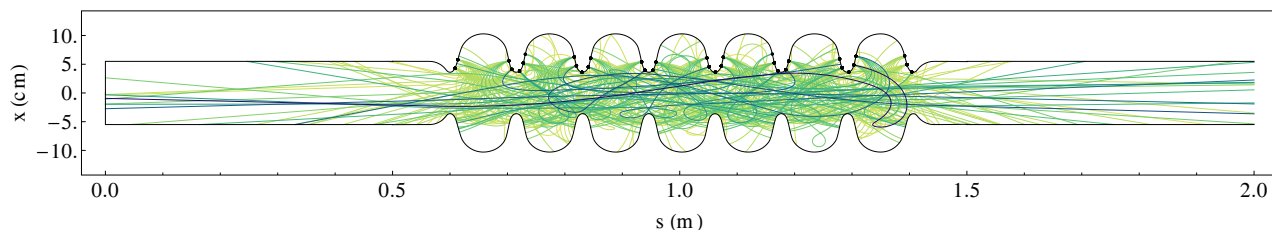


Figure 2: Sample particle tracks for field emitted electrons in a single Cornell ERL accelerating cavity, calculated using the Bmad time tracking module. Tracks are colored according to their final energy, with darker tracks having higher energies. The black dots indicate source points, which emit particles at various times. Approximately 500 tracks are shown. The electric and magnetic fields that influence these tracks are shown in Fig. 1.

emitters per unit area, and f_{rf} is the cavity oscillation frequency. Because these particles sample one period of cavity field oscillation, the average current that a test particle represents is $f_{rf} \cdot Q_n$.

Single SRF Cavity

The heart of the Cornell ERL consists of 7-cell cavities operating at 1.3 GHz, each designed to change the beam energy by 13 MeV. The electric field on the cavity wall, shown in Fig. 1a, is strongest at the irises. These regions are therefore the most likely points for field emission. Because of the exponential factor in Eq. (1), test particles representing extremely small charges can be produced. In order to conserve computing resources, we only keep particles representing charges within a certain factor of the maximum charge produced.

Figure 2 shows particle tracks from 34 emission points placed in the $x-s$ plane. More detailed distributions from tracking approximately 10^6 test particles are shown in Fig. 3. The vast majority of this current (99.5%) is lost within the cavity. The remainder escaping equally from the entrance and exit ends of the cavity.

Single Cryomodule

The standard Cornell ERL cryomodule contains 6 of these seven-cell cavities, as well as a single quadrupole magnet for beam focusing. Current losses along the length of the cryomodule are similar to Fig. 3a for each cavity. More interesting is the distribution of current for various energies, shown in Fig. 4a.

ERL Linac A

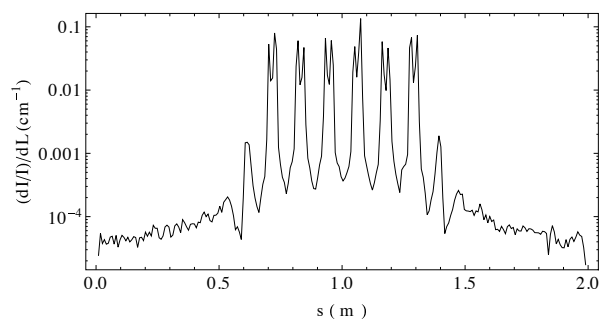
The two Cornell ERL linacs A and B consist of 35 and 29 of these cryomodules, respectively. Because they are very similar, we take Linac A as an example, with probability distributions shown in Fig. 4b as a function of energy. There we see that some particles can achieve high energy, but at relatively low probability. This is because the fields from the cryomodule quadrupole magnets tend to divert particles with energies much different from the (two) designed beam energies. This can be seen in the figure when all quadrupole magnets are turned off.

05 Beam Dynamics and Electromagnetic Fields

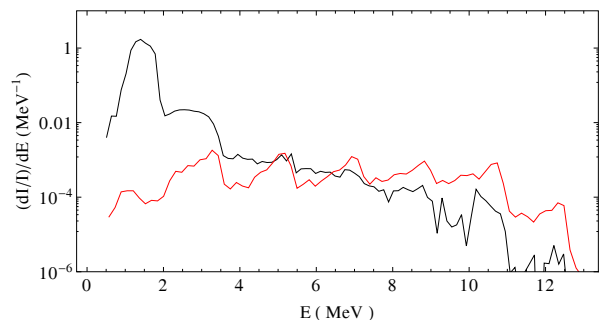
D02 Non-linear Dynamics - Resonances, Tracking, Higher Order

FUTURE WORK

Presently the tracking terminates when the particle encounters the wall of an element, so we plan to include a secondary emission model in our simulations based on results from the Monte Carlo code MCNPX [10]. Preliminary MCNPX calculations of the yield ratio and average energy of secondary electrons are shown in Fig. 5. Additionally, we plan to add distributions of emitter β_{FN} and A_{FN} to the dark current test particle creation program.



(a) Dark current loss distribution along the cavity length.



(b) Dark current loss distributions terminating in the cavity (black) and escaping the cavity (red), as a function of final energy.

Figure 3: Dark current distributions created in a single accelerating cavity, normalized by the total current. The peaks in Fig. 3a are located at the cavity irises. Parameters $\beta_{FN} = 100$, $A_{FN} = 10^{-11} \text{ cm}^2$, and $N_A = 0.1 \text{ cm}^{-2}$ were used in all simulations.

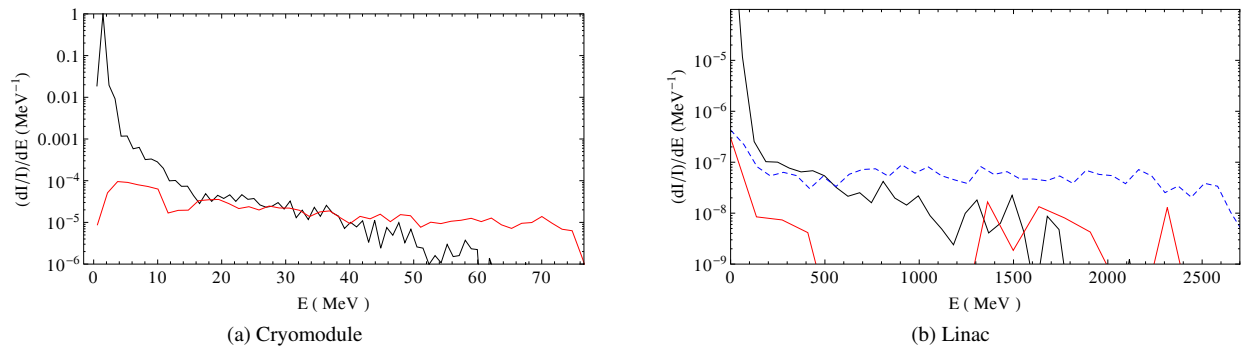
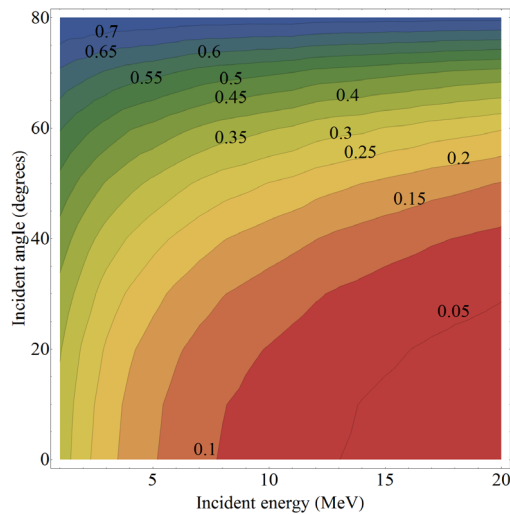
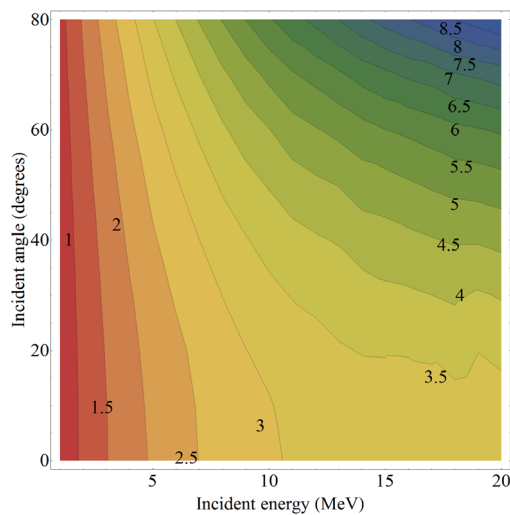


Figure 4: Dark current probability distributions as a function of final energy for a cryomodule and one of the two Corell ERL linacs. Similar to Fig. 3b, the red lines represent particles that escape the ends of these sections. The dashed blue line in Fig. 4b shows escaping particles from the linac with all quadrupole magnets turned off.



(a) Secondary electron yield ratio



(b) Average secondary electron kinetic energy (contours in MeV)

Figure 5: MCNPX [10] calculations of secondary electron yield ratios (reflected electron per incident electron) and their average energies, as a function of incoming energy and angle on a 3 mm thick slab of Nb.

ACKNOWLEDGEMENTS

The authors thank Nick Valles for providing the cavity field data. This work was supported by NSF award DMR-0807731.

REFERENCES

- [1] G. H. Hoffstaetter, S. Gruner, & M. Tigner, *eds.*, Cornell ERL Project Definition Design Report (2011)
<http://erl.chess.cornell.edu/PDDR>
- [2] V. Balandin *et al.*, “Studies of Electromagnetic Cascade Showers Development in the TESLA Main Linac Initiated by Electron Field Emission in RF Cavities,” TESLA Report 2003-10 (2003)
- [3] L. Fröhlich, “Machine Protection for FLASH and the European XFEL,” Ph.D. Dissertation, Universität Hamburg (2009)
- [4] J. Norem *et al.*, “Dark current, breakdown, and magnetic field effects in a multicell, 805 MHz cavity,” *Phys. Rev. ST- AB* **6**, 072001 (2003)
- [5] A. Temnykh, “Measurement of NdFeB permanent magnets demagnetization induced by high energy electron radiation,” *Nucl. Instr. and Meth. A* **515** 13-19 (2003)
- [6] H. Padamsee *RF Superconductivity*, Wiley-VCH (2009)
- [7] D. Sagan, “Bmad: A relativistic charged particle simulation library,” *Nuc. Instrum. and Methods in Phys Research A* **558**, 356–359 (2006).
<http://www.lepp.cornell.edu/~dcs/bmad>.
- [8] C. Chiu, “Dark Current Simulations for the Cornell ERL,” CLASSE REU report (2011)
- [9] A. Adelmann, Ch. Kraus, Y. Ineichen *et al.*, “The Object Oriented Parallel Accelerator Library (OPAL), Design, Implementation and Application,” *Proceedings of the 2009 Particle Accelerator Conference* (2009).
<http://amas.web.psi.ch/docs/>
- [10] J. S. Waters, *ed.*, “MCNPX Users Manual’ LA-UR-02-2607 (2002)
<http://mcnpx.lanl.gov/>